

## Carrier transport at the junction of tandem solar cells

N Palit, A Dasgupta, S Ray and P Chatterjee\*

Energy Research Unit, Indian Association<sup>1</sup> for the Cultivation of Science,  
Calcutta-700 032, India

E-mail : erpc2@mahendra.iacs.res.in

**Abstract** . Computer simulation of experimental current-voltage and spectral response characteristics of an incomplete cell structure  $-p_1-n_1-n_2$  has been used to understand the hole transport mechanisms at the  $n$ - $p$  junction. Two types of  $p$ -layer at the junction have been studied: (i) hydrogenated microcrystalline silicon ( $\mu\text{-Si:H}$ ) and (ii) hydrogenated amorphous silicon carbide ( $\text{a-SiC:H}$ ). Case (i) shows a fairly high fill factor (FF) and conversion efficiency ( $\eta$ ), as against a very low FF and  $\eta$  in case (ii). Modelling reveals that this difference is due to the much lower activation energy, hence, larger free hole population in  $p$ - $\mu\text{-Si:H}$ . We also learn that both tunnelling and diffusion help push holes produced in  $p$ , by the incident light, towards the recombination layer at the junction. Thus, to ensure high rate of diffusion of holes,  $p_2$  should have a high free hole density, which in turn, leads to improved performance. Preliminary studies on double junction solar cells reveal that a  $\mu\text{-Si:H}$   $p$ -layer at the junction results in an 8% improvement in FF.

**Keywords**  $p_1-n_1-n_2$  structure, simulation, transport mechanisms

**PACS Nos.** 85.30.De, 84.60.Jt

### 1. Introduction

The  $n^+/p^+$  junction between the individual subcells in a tandem solar cell structure, is characterised by a high reverse electric field, which tends to drive the carriers approaching it, in a direction opposite to the flow of carriers inside each subcell. These carriers being hindered to reach the junction from their respective subcells, may pile-up at the junction region and result in a reduction of the electric field in the individual subcells, yielding low open-circuit voltage ( $V_{oc}$ ) and fill factor (FF). It is therefore of utmost importance to ensure that electrons from the subcell on the  $n^+$  side, and holes from the subcell on the  $p^+$  side, can easily approach this junction and recombine with each other. For this purpose, a proper understanding of the mechanisms of carrier transport near this junction is essential.

Hou *et al* [1] suggested that a high-recombination layer (RL) should be incorporated at the  $n^+/p^+$  contact to ensure efficient recombination. Alternatively, the same objective could be achieved by making at least one of the  $n^+$ ,  $p^+$  layers microcrystalline [2]. It has also been suggested that electrons from the  $n^+$  side and holes from the  $p^+$  side partly "tunnel" towards this junction against the high opposing  $n^+/p^+$  field. Computer simulation of such tandem cell structures [1, 3] has shown that, to simulate the real tunneling of electrons and holes

respectively to the junction region, it is essential to grade the conduction band edge on the  $n^+$  side and valence band edge on the  $p^+$  side near the junction, to match the experimentally obtained high  $V_{oc}$  and FF of tandem solar cells. In this article, modelling of experimental current-voltage and quantum efficiency characteristics of thin film PINP structures has been used to understand the hole transport mechanisms at the  $n^+/p^+$  junction between two subcells of a tandem structure, to realise the relative importance of a particular carrier transport mechanism at the junction, when the  $p$ -layer here is (a)  $\text{a-SiC:H}$  and (b)  $\mu\text{-Si:H}$ , and, to discuss how the understanding of this mechanism may help us to improve the performance of tandem solar cells. For this study we have considered a PINP structure with two different types of  $p$ -layer at the junction: (i)  $p$ -type hydrogenated microcrystalline silicon ( $\mu\text{-Si:H}$ ) and (ii) hydrogenated amorphous silicon carbide ( $p\text{-a-SiC:H}$ ).

### 2. Simulation model

Our one-dimensional electrical-optical model [3, 4] solves the Poisson's equation and the two carrier continuity equations under steady-state conditions for the given semiconductor device structure and yields the current density-voltage characteristic and the quantum collection efficiency. The details of the electrical modelling part are given elsewhere [5,6]. The gap state model used in our calculation consists of the tail states

\* Corresponding Author

and two Gaussian distribution functions to simulate the deep dangling bond states. The junction between the p-i-n subcells of the stacked structure has been modelled by a heavily defective recombination layer with a reduced mobility gap. The tunnelling of carriers towards this region has been simulated by band edge grading. The generation term in the continuity equations has been calculated using an original semi-empirical model [7,8], that has been integrated into the modeling program [3, 4]. Both specular interference effects; and diffused reflectances and transmittances due to interface roughness are taken into account. The programme requires as input the values of the complex refractive indices of each layer of the device. These have been measured by spectroscopic ellipsometry at the Laboratoire de Physique des Interfaces et des Couches Minces (LPICM), Ecole Polytechnique, Palaiseau, France.

### 3. Experimental

The  $p_1-i_1-n_1-p_2$  and  $p_1-i_1-n_1-p_2-i_2-n_2$  structure devices were deposited onto transparent conducting oxide(TCO) – coated glass substrates in a conventional four chamber radio frequency (13.56 MHz) plasma enhanced chemical vapor deposition (PECVD) system (Glasstech Solar Inc., USA) provided with a load lock. The back contact metal is aluminium. The n-layer at the junction is microcrystalline, while the p-layer here is either p-a-SiC:H or p- $\mu$ c-Si:H. The window p-layer is p-a-SiC:H and all other layers are amorphous. The light insolated J-V characteristics of these devices were taken under AM1.5G radiation from a solar simulator (WACOM, USA). Quantum efficiency has been measured using a chopped monochromatic probe light (ASTM designation E1021-84, 1985).

### 4. Experimental results and simulation

Figure 1 compares the experimentally obtained J-V and QE characteristics of an incomplete cell structure –  $p_1-i_1-n_1-p_2$  – to the results of our computer simulation : (a), (b) : when  $p_2$  is p- $\mu$ c-Si:H and (c) when it is p-a-SiC:H. The input parameters used in our simulation model are described in Table 1. The major part of the p-a-SiC:H/i-a-Si:H band offset has been assumed [9] to lie on the conduction band side. On the other hand experimentalists have shown [10, 11] that the major part of the mobility gap

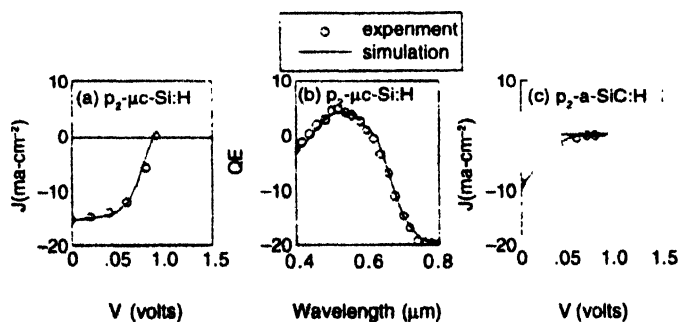


Figure 1. Experimentally obtained illuminated J-V and QE characteristics of thin film  $p_1-i_1-n_1-p_2$  structure devices (open circles) compared to the results from our model (solid lines) for two types of  $p_2$ -layer : (a) and (b) p- $\mu$ c-Si:H, (c) p-a-SiC:H.

offset between p- $\mu$ c-Si:H lies on the valence band side. In this study we have assumed for simplicity  $\Delta E_c = 0$ ,  $\Delta E_v = \Delta E_\mu$ . Except for the  $p_2$ -layer, all other layers are identical for the two cases. The reason for choosing such a structure for our study is the striking difference between the J-V characteristics in the two cases, with the structure containing p- $\mu$ c-Si:H at the junction showing fairly good J-V characteristics (Figure 1a) as against an extremely low FF and conversion efficiency ( $\eta$ ) when  $p_2$  is p-a-SiC:H (Figure 1c). The QE curve when  $p_2$  is amorphous, could not be obtained experimentally on account of the very low conversion efficiency of the device. For the  $p_1-i_1-n_1-p_2$  cases, the holes arriving at the junction are mainly those produced in  $p_2$ , which differ in nature. The  $n_1^+/p_2^+$  junction has been modelled by a highly defective RL with high capture cross-sections and a reduced band gap. The recombination between electrons from the top subcell and the holes from  $p_2$  (in the  $p_1-i_1-n_1-p_2$  structures) has been found from our calculations to be highest over the RL at the junction.

Table 1. Input parameters for the simulation model. The abbreviations are as follows : L : length of the layer ;  $\chi$  : electron affinity ;  $E_\mu$  : mobility band gap ;  $E_a$  : activation energy ;  $E_D$  ( $E_A$ ) : characteristic energy of the donor (acceptor) like tail states ; N : midgap density of states. The values of the neutral (charged) capture cross-sections have been taken to be  $10^{-16}$  ( $10^{-14}$ ) and electron (hole) mobility 20(4) in all the layers. When p-a-SiC:H is used after the recombination layer (i.e. in  $p_2$ -a-SiC:H) its thickness is 30 nm

Parameter	$p_2$ - $\mu$ c-Si:H	$p_1$ -a-SiC:H	i-a-SiC:H buffer	i-a-Si:H	$n_1$ - $\mu$ c-Si:H
L (nm)	30	10	5	360	30
$\chi$ (eV)	4.0	3.89	3.92	4.0	4.0
$E_\mu$ (eV)	1.54	2.0	1.96	1.86	1.6
$E_a$ (eV)	0.12	0.54	0.92	0.87	0.06
$E_D/E_A$ (meV)	30/20	130/70	90/55	50/30	30/2
N ( $\text{cm}^{-3}$ )	$1 \times 10^{18}$	$5 \times 10^{18}$	$5 \times 10^{16}$	$2 \times 10^{15}$	$1 \times 10^{16}$

### 5. Discussion

Figure 2 indicates that the band diagrams for the two cases of  $p_1-i_1-n_1-p_2$  structure are practically identical over the intrinsic

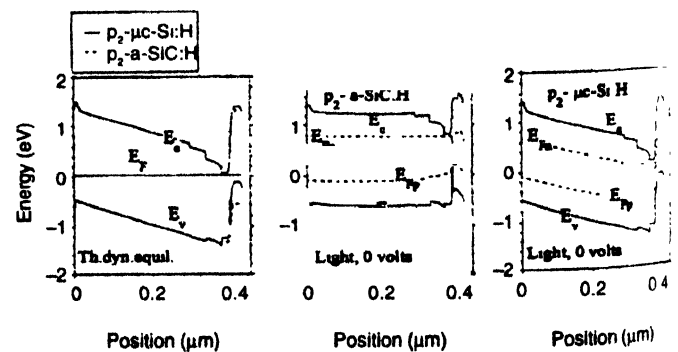


Figure 2. The band diagrams for  $p_1-i_1-n_1-p_2$  devices having two types of  $p_2$ -layer : p- $\mu$ c-Si:H and p-a-SiC:H, indicating that these are identical over the i-layer in thermodynamic equilibrium, but differ widely in the presence of light.

(1) layers, in thermodynamic equilibrium. But, they change markedly under illumination. For the device having  $p_2$ -a-SiC:H, the bands become almost flat, while the field over the i-layer remains high for the device with  $p_2$ - $\mu$ c-Si:H. Computer modelling indicates that the main difference in the two cases is the much higher free hole population (by  $\sim 7$  orders of magnitude) in  $p_2$  when it is microcrystalline (Figure 3a); which in turn, is a direct consequence of the low bulk activation energy ( $E_{ac} = 0.12$  eV) for this case as compared to  $E_{ac} = 0.54$  eV for  $p_2$ -a-SiC:H, measured experimentally. The Figure 3c indicates that the holes produced over the  $p_2$ -layer by illumination, move towards the RL at the junction ( $J_p$  is negative) and also that more holes can arrive at the junction region ( $J_p$  more negative), when  $p_2$  is  $\mu$ c-Si:H, than when it is amorphous. This results in higher recombination over the RL (Figure 3b) in the former case. We have found from our modelling that the RL at the junction must

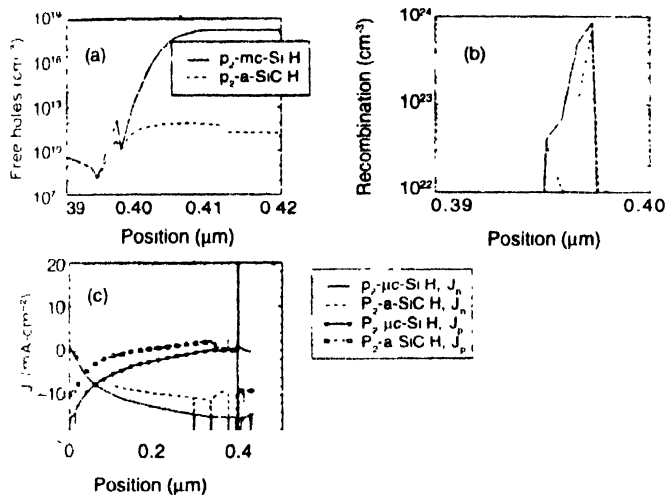


Figure 3. Computer generated plots of (a) the free hole density as a function of position over the RL and the  $p_2$ -layer; (b) the recombination over the RL and (c) the computer generated plots of the electron and hole current densities ( $J_n$  and  $J_p$  respectively), as a function of position in  $p_1$ - $i_1$ - $n_1$ - $p_1$  structure devices under AM1.5G light, having two different types of  $p_2$  layer:  $p_2$ - $\mu$ c-Si:H and  $p_2$ -a-SiC:H.

have a narrow mobility gap ( $E_\mu$ ) (in our case it is 1.0 eV) in order to match the experimentally obtained  $V_{oc}$  and FF. Such a narrow  $E_\mu$  reduces the potential barriers faced by carriers moving towards the  $n^+/p^+$  junction and simulates the real case tunnelling of carriers towards it, as has also been observed elsewhere [1,3]. No additional grading of the 30 nm  $p_2$ -layer (again, to simulate tunnelling of holes towards the  $n^+/p^+$  junction) was necessary to match the J-V and QE characteristics when  $p_2$  is microcrystalline, which, was however found essential to match the output characteristics when  $p_2$  is a-SiC:H. The reason for this is that  $\mu$ c-Si:H has a smaller band gap –  $E_\mu(p_2) = 1.54$  eV as compared to  $E_\mu(p_2) = 2.0$  eV for p-a-SiC:H. The potential barriers for holes moving towards the junction are therefore automatically reduced in the former case, without the need for additional tunnelling (additional valence band grading) to match the experimental results. However, the large electron – hole recombination in this region (Figure 3b), despite the high reverse

electric field at the junction, indicates that some counter mechanism must be there, which forces the holes towards the junction. Assuming that such a mechanism is the tunnelling of holes towards the junction alone, we would expect approximately the same negative hole current density over  $p_2$  in both the cases, since, (i) the RL has been assumed to have the same narrow band gap of 1.0 eV in both cases to simulate the tunnelling of carriers towards it, (ii) when  $p_2$  is a-SiC:H, additional grading of the valence band edge of  $p_2$  was performed, again to simulate the tunnelling of holes towards the RL, while in  $p_2$ - $\mu$ c-Si:H, the valence band offset automatically reduces the potential barriers for holes moving towards the RL, with approximately the same effect as the additional tunnelling described above for the  $p_2$ -a-SiC:H case. But the large difference in  $J_p$  for the two cases imply that there must be some other mechanism of hole transport towards the junction, and our modelling calculations clearly indicate that this is diffusion, due to concentration gradient, from a region of high free hole density ( $p_2$ ) to a region of low hole density ( $n_1$ ). This diffusion is considerably higher when  $p_2$  is microcrystalline due to its larger free hole population (Figure 3a). Thus when  $p_2$  is  $\mu$ c-Si:H, a larger number of holes compared to the case when  $p_2$  is a-SiC:H, are available for recombination with electrons arriving at the RL from  $i_1$ , there is no electron pile-up (Figure 4b), resulting in a higher electric field and lower recombination over the i-layer (Figures 4c, 4a), and hence good J-V characteristics (Figure 1a). The energy band diagram, therefore, retains a good slope over the i-layer under light, for this case (Figure 2). We may therefore conclude that in  $p_1$ - $i_1$ - $n_1$ - $p_2$  structure, diffusion plays a very important role in forcing holes towards the junction. This mechanism of hole transport may be augmented by choosing a  $p_2$ -layer with a high free hole density.

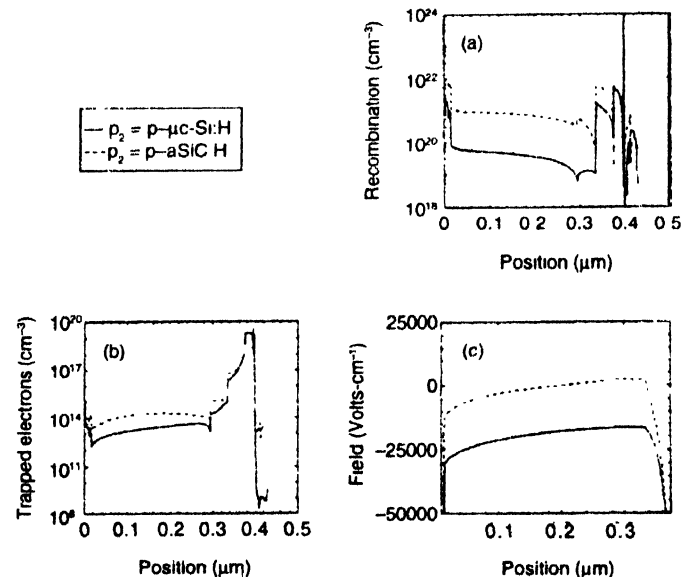


Figure 4. Computer generated plots of (a) the recombination and (b) the trapped electron population over the devices; (c) the electric field over  $i_1$ , under AM1.5G light, for  $p_1$ - $i_1$ - $n_1$ - $p_2$  structure devices having two different types of  $p_2$  layer:  $p_2$ - $\mu$ c-Si:H and  $p_2$ -a-SiC:H.

Preliminary work has been started to study the effect of the two types of p-layer at the junction :  $\mu\text{c-Si:H}$  and  $\text{a-SiC:H}$ , when applied in double junction solar cells.

## 6. Conclusions

Tunnelling and diffusion are the two mechanisms of hole transport towards the  $n^+/p^+$  junction of double junction solar cells. Tunneling as transport mechanism for holes towards the junction is more important when the p-layer at the junction is  $\text{a-SiC:H}$  than when it is microcrystalline, while diffusion play a more prominent role in the latter case. A p-layer at the junction with a high free hole density (low activation energy in the device) which gives rise to a high rate of diffusion of holes, has been shown to produce an all-round improvement in the case of

$p-i-n-p$  structure devices. Preliminary experimental results and their simulation (Figure 5) indicate that in double junction cells, a p-layer at the junction with a high free hole density ( $p\text{-}\mu\text{c-Si:H}$ ) produces a significant improvement in the fill factor of the device

## Acknowledgments

The work was carried out under a project funded jointly by the Ministry of Non-Conventional Energy Sources and the Department of Science and Technology, Government of India and the authors are grateful to the two departments for financial support. The authors are indebted to Dr. S. Hamma of the LPICM, Ecole Polytechnique, France, for measurements of the complex refractive indices of the boron doped microcrystalline films. They are also grateful to Prof. A. K. Barua of IACS, Calcutta, India for many useful discussions.

## References

- [1] J Y Hou, J K Arch, S J Fonash, S Wiedeman and M Bennet *Proceeding of the 22nd IEEE Photovoltaic Specialists' Conference* (Las Vegas, USA) vol. II 1260 (1991)
- [2] N Pellaton Vaucher, B Rech, D Fischer, S Dubail, M Goetz, H Keppner, N Wyrsh, C Beneking, O Hadjadj, V Shklover and A Shah *Sol. Energy Mater. Sol. Cells* **49** 27 (1997)
- [3] N Palit and P Chatterjee *Solar Energy Materials and Solar Cells* **53** 235 (1998)
- [4] P Chatterjee, F Leblanc, M Favre and J Perrin *Mater. Res. Soc. Symp. Proc.* **426** 593 (1996)
- [5] Parsathi Chatterjee *J. Appl. Phys.* **76** 1301 (1994)
- [6] Parsathi Chatterjee *J. Appl. Phys.* **79** 7339 (1996)
- [7] F Leblanc, J Perrin and J Schmitt *J. Appl. Phys.* **75** 1074 (1991)
- [8] F Leblanc *Thèse de Docteur en Science* (Université de Paris Sud Centre d'Orsay) (1992)
- [9] Z Y Wu, J M Siefert and B Equer *Proc. 10th European Photovoltaic Solar Energy Conference* (Lisbon, Portugal) p 953 (1991)
- [10] X Xu, J Yang, A Banerjee, S Guha, K Vasanth and S Wagner *Appl. Phys. Lett.* **67** 2323 (1995)
- [11] S Hamma and P Roca i Cabarrocas *Appl. Phys. Lett.* **74** 3218 (1999)

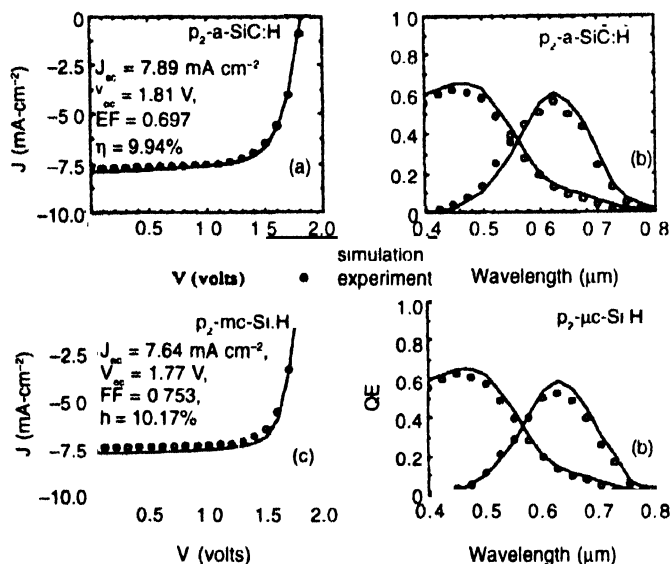


**Figure 5.** Experimentally obtained illuminated J-V and red- and blue-color light biased QE characteristics for  $p_1-i_1-n_1-p_2-i_2-n_2$  structure thin film double junction cells (open circles) compared to the results calculated on the basis of our model (solid lines) : (a) and (b) when the p-layer at the junction ( $p_2$ ) is  $\text{a-SiC:H}$ ; and (c) and (d) when it is  $\mu\text{c-Si:H}$ . The calculated values of  $J_{sc}$ ,  $V_{oc}$ , FF and  $\eta$  under AM1.5G light are shown on the J-V plots for the two types of  $p_2$ -layer